

1 **Perspective**

2 **Linking structure to function:**

3 **the connection between mesophyll structure and**  
4 **intrinsic water use efficiency**

5

6 Jeroen D.M. Schreel<sup>1,2,\*</sup>, Guillaume Théroux-Rancourt<sup>3</sup>, Adam B. Roddy<sup>1</sup>

7

8 <sup>1</sup>Institute of Environment, Department of Biological Sciences, Florida International  
9 University, Miami, FL., USA

10 <sup>2</sup>Plant Sciences Unit, Flanders Research Institute for Agriculture, Fisheries and Food (ILVO), B-  
11 9090 Melle, Belgium

12 <sup>3</sup>Biopterre - Bioproducts development center, Sainte-Anne-de-la-Pocatière, Québec, Canada

13

14 \*Corresponding author: Jeroen.Schreel@gmail.com

15

16 Contact information: J.D.M.S.: Jeroen.Schreel@gmail.com

17 ORCID: 0000-0002-6152-1307

18 G.T.R.: guillaume.theroux-rancourt@biopterre.com

19 ORCID: 0000-0002-2591-0524

20 A.B.R.: aroddy@fiu.edu

21 ORCID: 0000-0002-4423-8729

22 Conflicts of Interest: The authors declare no conflict of interest.

23

24 Author Contributions: Conceptualization and writing of the original draft was done by

25 J.D.M.S. Writing, reviewing and editing was done by G.T.R. and A.B.R.

26 The project was supervised by A.B.R.

27

28

29 Number of figures: 3

30 Figures in color: Fig. 2 and Fig. 3

31 Supplement: S1 References used in Fig. 2

32 S2 Fig. S1 and references used in Fig. S1

33 **Short summary**

34 Leaf mesophyll cells are often approximated by capsules and spheres to discuss structure-  
35 function relationships. These assumptions allow an easy assessments based on widely  
36 available 2D datasets of foliar tissue. However, this is a rough approximation of often  
37 irregularly shaped spongy mesophyll cells. We suggest to use more rare 3D assessments to  
38 provide corrections and functions to be used in 2D assessments, rather than scaling 2D  
39 analysis to 3D structures based on the assumption of ideal shapes.

40

41 **Abstract**

42 Climate change-driven drought events are becoming unescapable in an increasing number of  
43 areas worldwide. Understanding how plants are able to adapt to these changing  
44 environmental conditions is a non-trivial challenge. Physiologically, improving a plant's  
45 intrinsic water use efficiency ( $WUE_i$ ) will be essential for plant survival in dry conditions.  
46 Physically, plant adaptation and acclimatisation are constrained by a plant's anatomy. In  
47 other words, there is a strong link between anatomical structure and physiological function.  
48 Former research predominantly focussed on using 2D anatomical measurements to  
49 approximate 3D structures based on the assumption of ideal shapes, such as spherical  
50 spongy mesophyll cells. As a result of increasing progress in 3D imaging technology, the  
51 validity of these assumptions is being assessed, and recent research has indicated that these  
52 approximations can contain significant errors. We suggest to invert the workflow and use  
53 the less common 3D assessments to provide corrections and functions for the more widely  
54 available 2D assessments. By combining these 3D and corrected 2D anatomical assessments  
55 with physiological measurements of  $WUE_i$ , our understanding of how a plant's physical  
56 adaptation affects its function will increase and greatly improve our ability to assess plant  
57 survival.

58

59 **Keywords:**

60 functional plant anatomy, intercellular airspace, leaf anatomy, leaf functional traits, leaf  
61 structure, mesophyll, structure-function relations, water use efficiency

62 **Introduction**

63 An increasing number of climate change-driven drought events (IPCC, 2018) is pushing plant  
64 species to the limits of their climatic tolerance (Fitzpatrick *et al.*, 2008; Feeley *et al.*, 2020).  
65 This abiotic stressor is a major constraint for crop production, greatly affecting food security  
66 (Fahad *et al.*, 2017). Agriculture can attempt to breed more drought-tolerant cultivars, which  
67 can be classified as a guided form of adaptation. Natural migration of wild plants to areas  
68 with more favourable conditions might partially alleviate the impact of these abiotic  
69 stressors. Still, numerous species are unable to keep pace with these imposed environmental  
70 changes (e.g., Corlett & Westcott, 2013). Alternatively, plants under abiotic stress can try to  
71 acclimate or adapt (Corlett & Westcott, 2013) to deal with these new hydrological  
72 conditions.

73 Plant adaptation and acclimatisation can occur on different levels: genetic (Lauteri *et*  
74 *al.*, 1997; Roddy *et al.*, 2020), anatomy (Théroux-Rancourt *et al.*, 2021) and physiology (Shao  
75 *et al.*, 2008) (Fig. 1). These different levels can interact, with changes in genetics leading to  
76 anatomical and physiological changes. If these anatomical and physiological changes are  
77 favourable, they will result in higher survival rates (Maggio *et al.*, 2001), relatively enriching  
78 the genetic pool with these modifications, and so forth. If plants are unable to adjust or  
79 migrate, they are pushed to extinction because of newly imposed climatic conditions (Corlett  
80 & Westcott, 2013). Knowing which species are able to adjust and how these modifications  
81 manifest is essential to assess plant survival rates under climate change.

82 Physically, these changes are constrained by a plant's anatomy. In other words, there  
83 is a strong link between structure and function or anatomy and physiology, respectively,  
84 which amalgamates in the field of functional plant anatomy (Fig. 1). Mesophyll structure can  
85 affect multiple important traits, e.g., leaf hydraulics and light perception (Théroux-Rancourt  
86 & Gilbert, 2017; Théroux-Rancourt *et al.*, 2023). This Perspective article focuses on the  
87 construction of a leaf's mesophyll tissue and how this structure affects mesophyll  
88 conductance for water vapour and carbon dioxide out and into the leaf, respectively (Evans  
89 *et al.*, 2009; Earles *et al.*, 2018). While plants have some capacity for anatomical adaptation,  
90 the limits of these physical changes to improve carbon gain and reduce water loss during dry  
91 conditions remain poorly understood.

92

93 **Carbon gained and water lost**

94 As drought events increase in frequency and intensity (IPCC, 2018), improving a plant's  
95 intrinsic water use efficiency ( $WUE_i$ ;  $\mu\text{mol CO}_2\cdot(\text{mol H}_2\text{O})^{-1}$ ) will be essential to avoid harmful  
96 water shortages (Hentschel *et al.*, 2016).  $WUE_i$  is defined as the ratio of photosynthetic rate  
97 ( $A$ ;  $\mu\text{mol CO}_2\cdot\text{m}^{-2}\cdot\text{s}^{-1}$ ) to stomatal conductance ( $g_s$ ;  $\text{mol H}_2\text{O}\cdot\text{m}^{-2}\cdot\text{s}^{-1}$ ) (Eq. 1) (Osmond *et al.*,  
98 1980; Seibt *et al.*, 2008), thus combining the carbon and water cycles through stomatal  
99 conductance and the gaseous component of mesophyll conductance. In recent decades, the  
100 potential of mesophyll conductance ( $g_m$ ) to significantly affect carbon fixation and water loss  
101 has been recognized (Warren, 2008; Evans *et al.*, 2009; Bunce, 2016; Earles *et al.*, 2019).  
102 Furthermore,  $g_m$  is implicitly included in  $WUE_i$  as  $A$  is a function of  $g_s$  and  $g_m$  (Eq. 1). While  $g_s$   
103 determines how fast  $\text{CO}_2$  can enter the leaf through stomata,  $g_m$  determines how fast  $\text{CO}_2$   
104 can move from stomata to the chloroplast where it can be fixed as sugars during  
105 photosynthesis.

$$WUE_i = \frac{A}{g_s} \frac{f(g_s, g_m, \dots)}{f(g_s)} \quad \text{Eq. 1}$$

106  $g_m$  consists of the algebraic sum of its gaseous ( $g_{IAS}$ ; Eq. 2) and liquid ( $g_{liq}$ ; Eq. 3)  
107 components, the former denoting diffusion in the intercellular airspace (IAS) (Earles *et al.*,  
108 2018). The effect of the IAS structure on gas diffusion in the IAS is approximated by diffusion  
109 in a porous medium (Eq. 2) (Earles *et al.*, 2018).

$$g_{IAS} = \frac{\theta_{IAS} D_m}{0.5 L_{mes} \tau_{leaf} \lambda_{leaf}} \quad \text{Eq. 2}$$

110 where  $\theta_{IAS}$  is mesophyll porosity ( $\text{m}^3\cdot\text{m}^{-3}$ ),  $D_m$  is the diffusion coefficient of  $\text{CO}_2$  in air  
111 ( $\text{m}^2\cdot\text{s}^{-1}$ ),  $0.5L_{mes}$  is half the mesophyll thickness (m),  $\tau_{leaf}$  is the tortuosity factor ( $\text{m}^2\cdot\text{m}^{-2}$ ) and  
112  $\lambda_{leaf}$  is lateral path lengthening ( $\text{m}\cdot\text{m}^{-1}$ ).

113 Eq. 2 assumes that  $g_{IAS}$  is a function of foliar structure, yet each element of the  
114 equation does not depend on the same tissue or cell type. While  $\theta_{IAS}$  and  $\tau_{leaf}$  are a function  
115 of mesophyll tissue,  $\lambda_{leaf}$  is highly dependent on stomatal density (e.g. Earles *et al.*, 2018;  
116 Théroux-Rancourt *et al.*, 2023), clearly linking the spatial organization of both stomata and  
117 mesophyll cells to  $g_{IAS}$  and  $WUE_i$ .

118 In terms of functional plant anatomy, maximizing  $WUE_i$  entails an optimization  
119 problem where both a reduction in  $g_{IAS}$  for water vapor diffusion and an increase in  $g_{IAS}$  for

120  $\text{CO}_2$  diffusion are beneficial. As both pathways obviously overlap, it is unclear how a plant  
121 will physically optimise at the tissue level for dry conditions. Based on the diffusion  
122 coefficient of  $\text{CO}_2$  and water vapor in air of 0.158 and  $0.247 \text{ cm}^2 \cdot \text{s}^{-1}$  (at  $20^\circ\text{C}$ ), respectively, it  
123 can be hypothesized that reducing  $g_{\text{IAS}}$  would be more beneficial as the diffusion coefficient  
124 for water vapour is larger. This should result in a reduction of water loss that is more  
125 pronounced than the reduction in carbon gain, thus increasing  $\text{WUE}_i$ . However, if  $g_{\text{IAS}}$  does  
126 decrease, it is still unclear how different plant species would accomplish this. Is it more  
127 beneficial to increase  $\tau_{\text{leaf}}$  or decrease stomatal density, thus increasing  $\lambda_{\text{leaf}}$ ? Should  $\theta_{\text{IAS}}$   
128 increase or  $L_{\text{mes}}$  decrease? These are non-trivial questions which rely on the interplay of  
129 multiple variables. For example, sun leaves of *Fagus sylvatica* have been observed to have a  
130 higher  $g_{\text{IAS}}$  compared to shade leaves (Janová *et al.*, 2024), while sun leaves of *Vitis vinifera*  
131 indicated lower  $\theta_{\text{IAS}}$  and higher  $L_{\text{mes}}$  values compared to shade leaves, resulting in a lower  $g_{\text{IAS}}$   
132 (Thérroux-Rancourt *et al.*, 2023). Different tendencies could result from differences in species  
133 but could just as likely vary within the same species due to the interplay of multiple variables  
134 such as light intensity and hydration.

135

### 136 **Adding the third dimension**

137 *3D structure and  $\text{WUE}_i$*

138 As  $\text{WUE}_i$  is a function of  $g_m$ , structural features in mesophyll anatomy are expected to  
139 correlate with a plant's  $\text{WUE}_i$ . In coniferous species this resulted in a significant correlation  
140 between  $\text{WUE}_i$  and the number of stomata per unit of mesophyll volume (Trueba *et al.*,  
141 2022) (Fig. 2a), the number of stomata per unit of mesophyll surface area (Fig. 2b) and the  
142 number of stomata per unit of mesophyll intercellular airspace (Fig. 2c), but not the  
143 mesophyll surface area exposed to IAS per unit of total leaf area ( $S_m$ ; Fig. 2d). While also  
144 significant correlations between  $\text{WUE}_i$  and vein-based variables were found (Trueba *et al.*,  
145 2022), these observations suggest that stomatal density and variables based on mesophyll  
146 area, volume and porosity could be some of the major drivers for  $\text{WUE}_i$ .

147 Even though stomatal density is the major component of  $g_s$ , stomatal size also has a  
148 significant impact on  $g_s$ , and inversely on a plant's estimated water use efficiency (Liu *et al.*,  
149 2016). As stomatal density and stomatal size covary (Jordan *et al.*, 2020), a simplified  
150 assessment can be performed by investigating one of these parameters, but a stronger

151 relationship is expected when using stomatal area fraction (Liu *et al.*, 2016), defined as the  
152 product of stomatal density and stomatal size, divided by leaf area. In terms of adaptation to  
153 aridity, stomatal density appears to be the dominant factor over stomatal size (Liu *et al.*,  
154 2016). When stomatal densities scaled by mesophyll variables decrease,  $WUE_i$  increases (Fig.  
155 2a-c). This could be the result of a decreased  $g_{IAS}$ , combined with a larger diffusion coefficient  
156 for water vapor compared to  $CO_2$  in air. However, based on these data it is unclear whether  
157 stomatal density or mesophyll structure has the strongest influence on  $WUE_i$ . Stomatal  
158 density predominantly affects  $\lambda_{leaf}$ , with a decrease in stomatal density leading to an  
159 increase in  $\lambda_{leaf}$  (Earles *et al.*, 2018). However, mesophyll cell size has been linked to  $CO_2$   
160 diffusion inside leaves (Théroux-Rancourt *et al.*, 2021), suggesting that the interaction  
161 between stomatal density and mesophyll structure is driving  $WUE_i$ , as has been indicated by  
162 Lundgren *et al.* (2019), and not one or the other.

163 Significant changes in mesophyll structure as a result of varying environmental  
164 conditions, such as light and water availability (Théroux-Rancourt & Gilbert, 2017;  
165 Momayyezi *et al.*, 2022; Théroux-Rancourt *et al.*, 2023), have been observed. Drought can  
166 result in a decreased mesophyll cell volume, in turn causing an increase in  $\theta_{IAS}$  and  $g_{IAS}$   
167 (Momayyezi *et al.*, 2022). However, whether the effect of drought amplifies or reduces the  
168 effect of increased light interception through interactive effects, such as reduced light  
169 absorption due to drought (Momayyezi *et al.*, 2022), remains unclear. Furthermore, as  
170 structural variables are interlinked, different anatomical changes might result in the same  
171 physiological optimum, e.g., (i) a decrease in  $\theta_{IAS}$  could alleviate the effect of a decrease in  
172  $L_{mes}$  and (ii) an increase in  $\tau$  or  $\lambda$  can have similar effects with respect to  $g_{IAS}$ . To add to this  
173 complexity, some of these changes might rely on 3D directional structures (Harwood *et al.*,  
174 2021) rather than single-leaf variables.

175

## 176 *Errors based on 2D assessments*

177 Palisade and spongy mesophyll cells have often been approximated by capsules and spheres,  
178 respectively, to discuss structure-function relationships (Nobel, 2020). However, this is a  
179 rough approximation as spongy cells are often irregularly shaped (Haberlandt, 1904;  
180 Théroux-Rancourt *et al.*, 2020b; Borsuk *et al.*, 2022). These assumptions have been  
181 advantageous as they allowed easy assessments based on widely available 2D datasets of

182 foliar tissue and required low processing power. However, as we are entering a new era  
 183 where 3D observations are becoming more common and processing power is rarely limiting  
 184 for this type of research, the validity of 2D approximations for 3D traits such as  $\theta_{IAS}$ ,  $\tau_{leaf}$  and  
 185  $\lambda_{leaf}$  should be investigated, especially with respect to the irregular cell shape of spongy  
 186 mesophyll. Furthermore, these traits can exhibit high spatial heterogeneity (Earles *et al.*,  
 187 2018), making  $\tau_{leaf}$  directional rather than encompassing (Harwood *et al.*, 2021), and can  
 188 strongly influence  $g_{IAS}$  (Earles *et al.*, 2018).

189 During recent years, advances in methods for high-resolution 3D anatomical  
 190 observations, such as, confocal microscopy, multiphoton laser scanning microscopy (Wuyts  
 191 *et al.*, 2010), serial block-face scanning electron microscopy (SBF-SEM) (Harwood *et al.*,  
 192 2020), nuclear magnetic resonance (NMR) and X-ray computed microtomography (microCT)  
 193 (Brodersen & Roddy, 2016; Earles *et al.*, 2018, 2019; Mathers *et al.*, 2018) combined with  
 194 full-stack tissue segmentations based on machine learning (Théroux-Rancourt *et al.*, 2020a;  
 195 Rippner *et al.*, 2022), specialized software (Barbier de Reuille *et al.*, 2015) and other  
 196 pipelines (Wuyts *et al.*, 2010), have bloomed leading to new insights and the unravelling of  
 197 errors based on former 2D approaches. This type of research has indicated that including 3D  
 198 data of  $\tau_{leaf}$  and  $\lambda_{leaf}$  reduced the estimates of  $g_{IAS}$  based on anatomy, on average, by 37% in  
 199 bromeliad species (Earles *et al.*, 2018). Furthermore, 2D leaf sections underestimated the  
 200 mesophyll surface area exposed to IAS per unit of total leaf area ( $S_m$ ), in some cases leading  
 201 to errors of almost 50% compared to 3D microCT images (Théroux-Rancourt *et al.*, 2017;  
 202 Mathers *et al.*, 2018). This error can affect the assessment of other variables as  $S_m$  closely  
 203 correlates with A (Théroux-Rancourt *et al.*, 2017) and  $g_{liq}$  (Eq. 3) (Théroux-Rancourt *et al.*,  
 204 2021). Evans *et al.* (2009), for example, indicated that leaves with a large photosynthetic  
 205 capacity ( $P_c \sim f(A) \sim f(WUE_i)$ ) tend to increase  $g_m$  by increasing the surface area of chloroplast  
 206 exposed to IAS ( $S_c \sim f(S_m)$ ), clearly denoting the interlinkage between  $S_m$  and other variables  
 207 and the possibility of cascading errors due to 2D assessments.

$$g_{liq} = \frac{\frac{SA_{mes}}{V_{mes}} \times \frac{S_c}{S_m}}{R} \quad \text{Eq. 3}$$

208 where  $SA_{mes}$  is the mesophyll surface area exposed to IAS ( $m^2$ ),  $V_{mes}$  is the mesophyll  
209 volume ( $m^3$ ) and R is a combination of different resistance components of the liquid diffusion  
210 path through mesophyll cells ( $m^2 \text{ chloroplast.s.mol}^{-1}$ ), including diffusion through cell walls.

211 While a lot of variation exists in the relation between  $S_c$  and  $S_m$  (Fig. S1), an error in  $S_m$   
212 will not directly affect  $S_c S_m^{-1}$  as this term is generally estimated as a ratio, e.g.  $0.73 \pm 0.01$   
213 (mean  $\pm$  SE; Fig. S1). However,  $S_m$  is  $SA_{mes}$  scaled per unit of leaf area (LA). As a consequence,  
214 errors in  $S_m$  will result in errors of  $SA_{mes}/V_{mes}$ . Based on the 3D dataset available in Trueba *et*  
215 *al.*, (2022), a significant ( $p < 0.001$ ) logarithmic relation between  $S_m$  and  $SA_{mes}/V_{mes}$  can be  
216 observed (Fig. 3). This makes sense as  $SA_{mes}/LA \sim SA_{mes}/V_{mes}$  corresponds to  $1/LA \sim 1/V_{mes}$ .  
217 However, when using 2D data from Hogan *et al.* (1994) and Vyas *et al.* (2007), no significant  
218 trend could be found. It is important to note that sample sizes are small and that the 2D  
219 dataset is based on broadleaved species, while the 3D dataset is based on coniferous  
220 species. As such, part of the observed difference could thus be ascribed to statistical errors  
221 and species diversity; however, it is expected that a significant amount of difference  
222 originated from errors in 2D anatomical assessments of 3D structures.

223

## 224 **A way forward**

225 Despite its increasing use in publications, 3D methods are still not universally available. The  
226 main goal of 3D methods should be to provide corrections and adaptations for the more  
227 widely available 2D methods. One such adaptation is determining the number of 2D slices  
228 needed to make an acceptable approximation of  $S_m$  (Théroux-Rancourt *et al.*, 2017), or  
229 providing an equation that encompasses the 3D reality of leaves but uses readily available  
230 2D data (Earles *et al.*, 2018). Furthermore, knowledge gained from 3D anatomical  
231 assessments must eventually be shaped in a way that allows the use of lower dimensional  
232 data for upscaling, e.g., from 2D leaves to canopy-level models (Earles *et al.*, 2019).

233 We suggest to use 3D assessments to provide corrections and functions to be used in  
234 2D assessments rather than scaling 2D analysis to 3D structures based on the assumption of  
235 ideal shapes such as spherical spongy mesophyll cells. Furthermore, by improvements in  
236 computational power and advancements in 3D structural assessment methods, the potential  
237 for new avenues in the field of functional plant anatomy is increasing drastically. By  
238 combining corrected 3D anatomical assessment with physiological measurements, our

239 understanding of how a plant's physical adaptation affects its function increases and will  
240 greatly improve our ability to assess plant survival.

241 **Data Availability Statement**

242 No original data are used in this perspective.

243

244 **Funding**

245 This work was supported by the NSF grant CMMI-2029756 to JDMS.

246 **References**

247 Barbier de Reuille P, Routier-Kierzkowska A-L, Kierkowski D, Bassel GW, Schüpbach T,  
248 Tauriello G, Bajpai N, Strauss S, Weber A, Kiss A, *et al.* 2015. MorphoGraphX: A platform  
249 for quantifying morphogenesis in 4D. *eLife* 4: Article: e05864.

250 Borsuk AM, Roddy AB, Théroux-Rancourt G, Brodersen CR. 2022. Structural organization  
251 of the spongy mesophyll. *New Phytologist* 234: 946–960.

252 Brodersen CR, Roddy AB. 2016. New frontiers in the three-dimensional visualization of plant  
253 structure and function. *American Journal of Botany* 103: 184–188.

254 Bunce J. 2016. Variation among soybean cultivars in mesophyll conductance and leaf water  
255 use efficiency. *Plants* 5: Article: 44.

256 Corlett RT, Westcott DA. 2013. Will plant movements keep up with climate change? *Trends*  
257 in *Ecology & Evolution* 28: 482–488.

258 Earles JM, Buckley TN, Brodersen CR, Busch FA, Cano JF, Choat B, Evans JR, Farquhar  
259 GD, Harwood R, Huynh M, *et al.* 2019. Embracing 3D complexity in leaf carbon–water  
260 exchange. *Trends in Plant Science* 24: 15–24.

261 Earles JM, Théroux-Rancourt G, Roddy AB, Gilbert ME, McElrone AJ, Brodersen CR. 2018.  
262 Beyond porosity: 3D leaf intercellular airspace traits that impact mesophyll conductance.  
263 *Plant Physiology* 178: 148–162.

264 Evans JR, Kaldenhoff R, Genty B, Terashima I. 2009. Resistances along the CO<sub>2</sub> diffusion  
265 pathway inside leaves. *Journal of Experimental Botany* 60: 2235–2248.

266 Fahad S, Bajwa AA, Nazir U, Anjum SA, Farooq A, Zohaib A, Sadia S, Nasim W, Adkins S,  
267 Saud S, *et al.* 2017. Crop Production under Drought and Heat Stress: Plant Responses and  
268 Management Options. *Frontiers in Plant Science* 8: Article: 1147.

269 Feeley KJ, Bravo-Avila C, Fadrique B, Perez TM, Zuleta D. 2020. Climate-driven changes in  
270 the composition of New World plant communities. *Nature Climate Change* 10: 965–970.

271 Fitzpatrick MC, Gove AD, Sanders NJ, Dunn RR. 2008. Climate change, plant migration, and  
272 range collapse in a global biodiversity hotspot: the *Banksia* (Proteaceae) of Western Australia.  
273 *Global Change Biology* 14: 1–16.

274 Haberlandt G. 1904. *Physiologische pflanzenanatomie*. Leipzig, Germany: W. Engelmann.

275 Harwood R, Goodman E, Gudmundsdottir M, Huynh M, Musulin Q, Song M, Barbour MM.  
276 2020. Cell and chloroplast anatomical features are poorly estimated from 2D cross-sections.  
277 *New Phytologist* 225: 2567–2578.

278 Harwood R, Théroux-Rancourt G, Barbour MM. 2021. Understanding airspace in leaves: 3D  
279 anatomy and directional tortuosity. *Plant, Cell & Environment* 44: 2455–2465.

280 Hentschel R, Hommel R, Poschenrieder W, Grote R, Holst J, Biernath C, Gessler A, Priesack  
281 E. 2016. Stomatal conductance and intrinsic water use efficiency in the drought year 2003: a  
282 case study of European beech. *Trees* 30: 153–174.

283 Hogan KP, Smith AP, Aruis JL, Saavedra A. 1994. Ecotypic differentiation of gas exchange  
284 responses and leaf anatomy in a tropical forest understory shrub from areas of contrasting  
285 rainfall regimes. *Tree Physiology* 14: 819–831.

286 IPCC. 2018. *Global Warming of 1.5°C. An IPCC Special Report on the impacts of global  
287 warming of 1.5°C above pre-industrial levels and related global greenhouse gas emission  
288 pathways, in the context of strengthening the global response to the threat of climate change,  
289 sustainable development, and efforts to eradicate poverty*.

290 Janová J, Kubásek J, Grams TEE, Zeisler-Diehl V, Schreiber L, Šantrůček J. 2024. Effect of  
291 light-induced changes in leaf anatomy on intercellular and cellular components of mesophyll  
292 resistance for CO<sub>2</sub> in *Fagus sylvatica*. *Plant Biology*.

293 Jordan GJ, Carpenter RJ, Holland BR, Beeton NJ, Woodhams MD, Brodribb TJ. 2020. Links  
294 between environment and stomatal size through evolutionary time in Proteaceae. *Proceedings*  
295 *of the Royal Society B* 287: Article: : 20192876.

296 Lauteri M, Scartazza A, Guido MC, Brugnoli E. 1997. Genetic variation in photosynthetic  
297 capacity, carbon isotope discrimination and mesophyll conductance in provenances of  
298 *Castanea sativa* adapted to different environments. *Functional Ecology* 11: 675–683.

299 Liu C, He N, Zhang J, Li Y, Wang Q, Sack L, Yu G. 2016. Variation of stomatal traits from  
300 cold temperate to tropical forests and association with water use efficiency. *Functional*  
301 *Ecology* 32: 20–28.

302 Lundgren MR, Mathers A, Baillie AL, Dunn J, Wilson MJ, Hunt L, Pajor R, Fradera-Soler M,  
303 Rolfe S, Osborne CP, *et al.* 2019. Mesophyll porosity is modulated by the presence of  
304 functional stomata. *Nature Communications* 10: Article: 2825.

305 Maggio A, Hasegawa PM, Bressan RA, Consiglio MF, Joly RJ. 2001. Unravelling the  
306 functional relationship between root anatomy and stress tolerance. *Australian Journal of*  
307 *Plant Physiology* 28: 999–1004.

308 Mathers AW, Hepworth C, Baillie AL, Sloan J, Jones H, Lundgren MR, Fleming AJ, Mooney  
309 SJ, Sturrock CJ. 2018. Investigating the microstructure of plant leaves in 3D with lab-based  
310 X-ray computed tomography. *Plant Methods* 14: Article: 99.

311 Momayyezi M, Borsuk AM, Brodersen CR, Gilbert ME, Théroux-Rancourt G, Kluepfel DA,  
312 McElrone AJ. 2022. Desiccation of the leaf mesophyll and its implications for CO<sub>2</sub> diffusion  
313 and light processing. *Plant, Cell & Environment* 45: 1362–1381.

314 Nobel PS. 2020. *Physiochemical and environmental plant physiology*. Cambridge, UK:  
315 Academic Press.

316 Osmond CB, Björkman O, Anderson DJ. 1980. *Physiological processes in plant ecology*.  
317 Springer.

318 Rippner DA, Raja PV, Earles JM, Momayyezi M, Buchko A, Duong FV, Forrestel EJ,  
319 Parkinson DY, Shackel KA, Neyhart JL, *et al.* 2022. A workflow for segmenting soil and  
320 plant X-ray computed tomography images with deep learning in Google's Colaboratory.  
321 *Frontiers in Plant Science* 13: Article: 893140.

322 Roddy AB, Théroux-Rancourt G, Abbo T, Benedetti JW, Brodersen CR, Castro M, Sastro S,  
323 Gilbride AB, Jensen B, Jiang G-F, *et al.* 2020. The scaling of genome size and cell size limits  
324 maximum rates of photosynthesis with implications for ecological strategies. *International*  
325 *Journal of Plant Sciences* 181: 75–87.

326 Seibt U, Rajabi A, Griffiths H, Berry JA. 2008. Carbon isotopes and water use efficiency:  
327 sense and sensitivity. *Oecologia* 155: 441–454.

328 Shao H-B, Chu L-Y, Jaleel CA, Zhao C-X. 2008. Water-deficit stress-induced anatomical  
329 changes in higher plants. *Comptes Rendus Biologies* 331: 215–225.

330 Théroux-Rancourt G, Earles JM, Gilbert ME, Zwieniecki MA, Boyce CK, McElrone AJ,  
331 Brodersen CR. 2017. The bias of a two-dimensional view: comparing two-dimensional and  
332 three-dimensional mesophyll surface area estimates using noninvasive imaging. *New*  
333 *Phytologist* 215: 1609–1622.

334 Théroux-Rancourt G, Gilbert ME. 2017. The light response of mesophyll conductance is  
335 controlled by structure across leaf profiles. *Plant, Cell & Environment* 40: 726–740.

336 Théroux-Rancourt G, Herrera JC, Voggendorf K, De Berardinis F, Luijken N, Nocker L, Savi  
337 T, Scheffknecht S, Schneck M, Tholen D. 2023. Analyzing anatomy over three dimensions  
338 unpacks the difference in mesophyll diffusive area between sun and shade *Vitis vinifera*  
339 leaves. *AoB Plants* 15: Article: plad001.

340 Théroux-Rancourt G, Jenkins MR, Brodersen CR, McElrone AJ, Forrestel EJ, Earles JM.  
341 2020a. Digitally deconstructing leaves in 3D using X-ray microcomputed tomography and  
342 machine learning. *Applications in Plant Sciences* 8: Article: e11380.

343 Théroux-Rancourt G, Roddy AB, Earles JM, Gilbert ME, Zwieniecki MA, Boyce CK, Tholen  
344 D, McElrone AJ, Simonin KA, Brodersen CR. 2021. Maximum CO<sub>2</sub> diffusion inside leaves is  
345 limited by the scaling of cell size and genome size. *Proceedings of the Royal Society B* 288:  
346 Article: 20203145.

347 Théroux-Rancourt G, Voggendorf K, Tholen D. 2020b. Shape matters: the pitfalls of  
348 analyzing mesophyll anatomy. *New Phytologist* 225: 2239–2242.

349 Trueba S, Théroux-Rancourt G, Earles JM, Buckley TN, Love D, Johnson DM, Brodersen  
350 CR. 2022. The 3D construction of leaves is coordinated with water use efficiency in conifers.  
351 *New Phytologist* 233: 851–861.

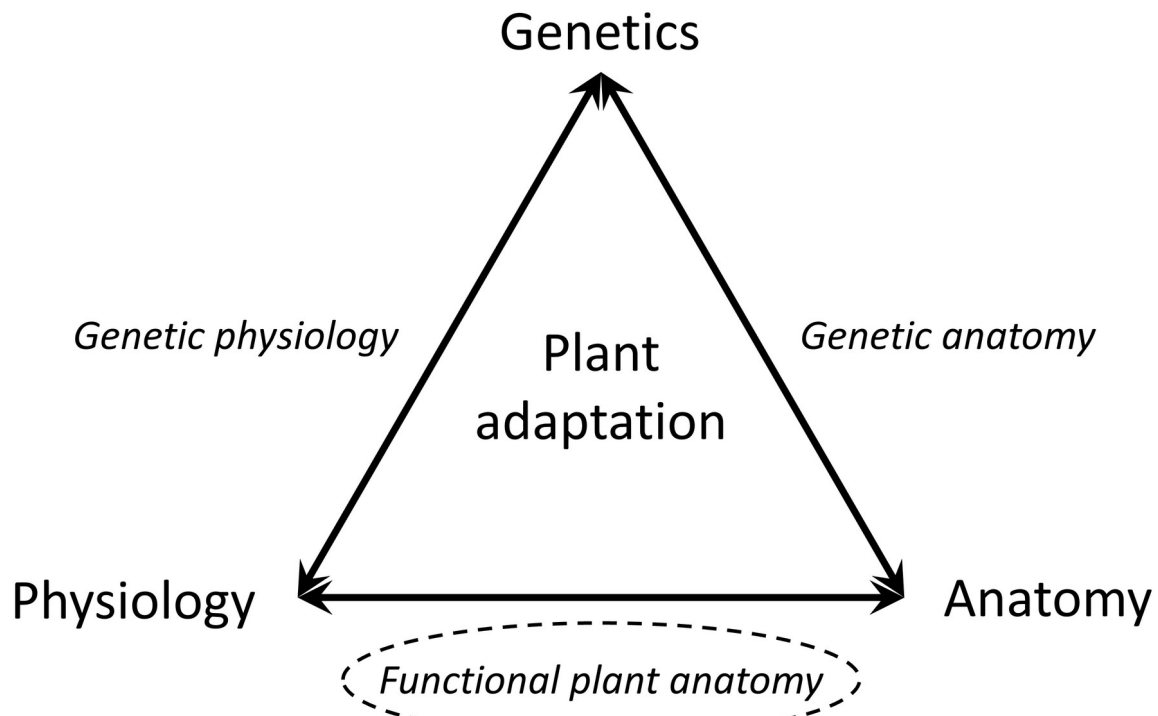
352 Vyas P, Bisht MS, Miyazawa S-I, Yano S, Noguchi K, Terashima I, Funayama-Noguchi S.  
353 2007. Effects of polyploidy on photosynthetic properties and anatomy in leaves of *Phlox*  
354 *drummondii*. *Functional Plant Biology* 34: 673–682.

355 Warren CR. 2008. Stand aside stomata, another actor deserves centre stage: the forgotten role  
356 of the internal conductance to CO<sub>2</sub> transfer. *Journal of Experimental Botany* 59: 1475–1487.

357 Wuyts N, Palauqui J-C, Conejero G, Verdeil J-L, Granier C, Massonnet C. 2010. High-  
358 contrast three-dimensional imaging of the *Arabidopsis* leaf enables the analysis of cell  
359 dimensions in the epidermis and mesophyll. *Plant Methods* 6: Article: 17.

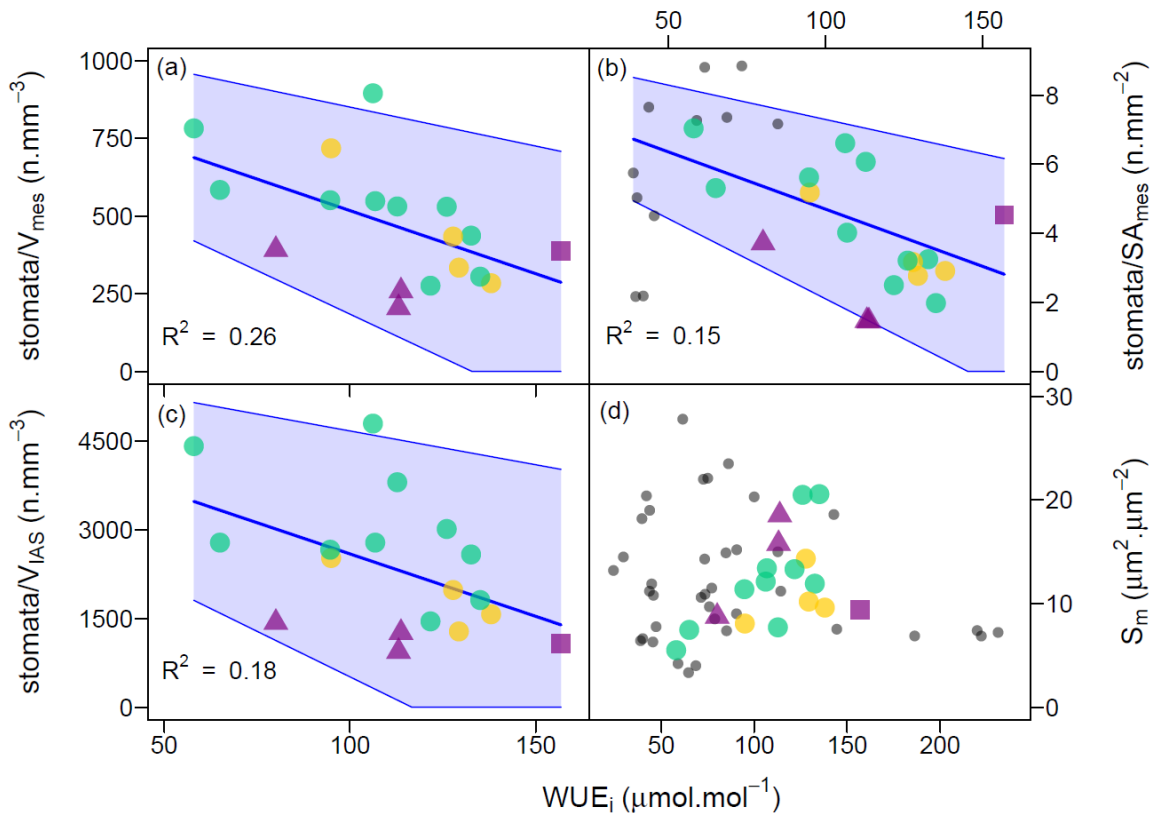
360

361 **Figure legends**



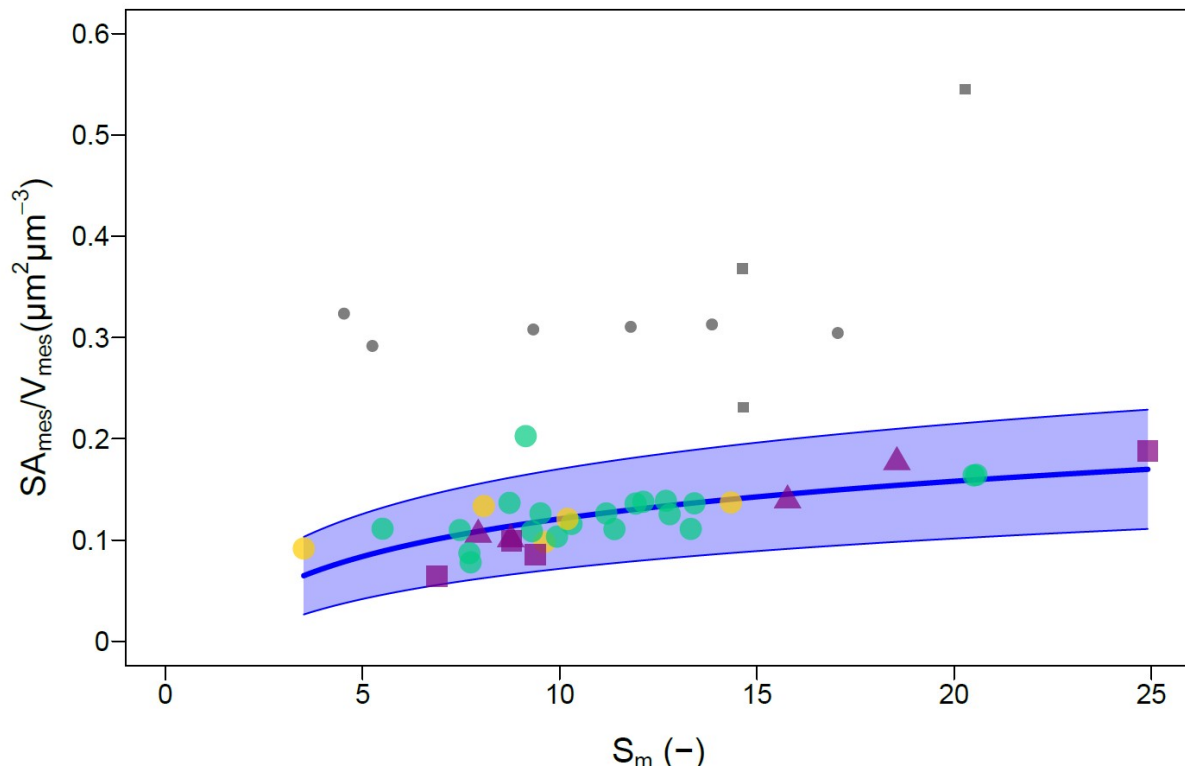
362

363 Fig. 1 Three main fields of plant sciences that can assess different aspects of plant  
364 adaptation: genetics, anatomy and physiology. The interaction of these fields creates  
365 subfields. In this Perspective, the subfield of functional plant anatomy is being proposed as a  
366 promising way forward to better understand plant adaptations.



367

368 Fig. 2 Physiological leaf traits as a function of intrinsic water use efficiency ( $\text{WUE}_i$ ). (a)  
 369 Number of stomata per unit of mesophyll volume ( $\text{stomata}/V_{\text{mes}}$ ); (b) Number of stomata per  
 370 unit of mesophyll surface area ( $\text{stomata}/SA_{\text{mes}}$ ); (c) Number of stomata per unit of mesophyll  
 371 intercellular airspace volume ( $\text{stomata}/V_{\text{IAS}}$ ); (d) Mesophyll surface area per unit of total leaf  
 372 area ( $S_m$ ). Solid blue regression lines and SE (shaded areas) are included. Coefficients of  
 373 determination are included. All fits have a p-value < 0.05. *Pinus* species from the subgenera  
 374 *Pinus* (green) and *Strobus* (yellow), along with other conifer species (purple), are indicated.  
 375 Species bearing flat leaves (square), flattened needle leaves (triangles), and needle-like  
 376 leaves (circles) are also identified (data from the supplement of Trueba *et al.* (2022)). Grey  
 377 circles represent data from other references (see supplementary information).



378

379 Fig. 3 Ratio of the mesophyll surface area exposed to IAS to the mesophyll volume  
 380 ( $SA_{mes}/V_{mes}$ ) as a function of mesophyll surface area exposed to the intercellular air space per  
 381 unit of total leaf area ( $S_m$ ). 3D data (in colour) based on X-ray microCT imaging (Trueba *et al.*,  
 382 2022), 2D data based on light microscopy (grey circles: Hogan *et al.* (1994); grey squares:  
 383 Vyas *et al.* (2007)). Blue line indicates a logarithmic fit to 3D colour data with the shaded  
 384 area visualizing the standard error of the fit ( $p < 0.001$ ).